

**DET MORPH – a new method for an accurate acquisition of
fine-morphological data –
Exemplified on the *Achillea millefolium* group (Asteraceae)**

Johannes Saukel*¹, Wolfgang Wlach¹

¹ Department of Pharmacognosy, University of Vienna, Althanstrasse 14, A-1090,
Vienna, Austria

Abstract

Det_Morph is a new approach for a detailed morphological analysis of primary segments of leaflets and ray florets from some species of the *Achillea millefolium* group (Asteraceae). 56 features of primary segments and 21 features of ray florets both in two different transformation types are yielded by the new software. The usefulness of these features is shown on data of 616 specimens of *Achillea setacea*, *A. collina*, *A. ceretanica*, *A. distans* s.l., *A. millefolium* s.l. and *A. pannonica*.

Key words

Achillea, computer aided analysis, morphology, analysis of shape & size.

Introduction

One of the major goals of pharmacognostical research is a precise description of medicinal plants and herbal drugs. Within the scope of our studies on Herba Millefolii (derived from species of the genus *Achillea* (Asteraceae)) we indicated that the shape and to a lesser extent the size of primary segments (called **leaflets**) of upper stem leaflets and of the ray florets are important characteristics for each taxon [1,2]. Traditionally used features, e.g. breadth and length of **leaflets** or of ligule (ray florets) are not sufficient for the description of the respective parts. In [3] the product from breadth and length was used as an approximate value for the area of **leaflets** etc. The first reason for the development of a special software was the striving for the proper evaluation of the area and the perimeter of **leaflets** and of ray florets (or parts of them). A first report was given in [4], and test applications are

given in [5 – 9]. A further advantage is the electronic availability of detailed drawings of interesting parts of the plants, particularly with regard to the large number of investigated material.

Functional principle

The software was written in **GFA-Basic®** for **Atari-computer®** and is also running under **Windows 98, 2000, XP®** and higher with the software emulation **MagiC_PC®**.

In the following only those parts of the **DET_MORPH** algorithm are described in detail which are necessary to yield the new features:

- 1a)** The creation of sample drawings using a microscope with drawing apparatus, after this the use of a scanner or a digital camera to get a bitmap.
- 1b)** The use of a digital camera for a shoot from the microscope.
Both methods supply a bitmap (rgb). The pictures must be transformed into a two color bitmap. Only this can be processed by the algorithm.
- 2)** Conversion from the bitmap into a vector graph which can be resized (extraction of the outline, cp. **fig. 1.**).
- 3)** Input a standard (length or breadth) for the pictured object.
- 4)** Resize the vector to a proper dimension (so all details can be seen on the screen).
- 5)** Define characteristic points onto the vector (e.g. begin and end of the ultimate segment of a leaflet, see **fig. 3.**).
- 6)** Automatic measurement of the vector and output/save of the computed values. A list of the new features in **tab. 1.** and **2..**

Ad 1) The method of choice is **1a.** It takes more time than **1b,** however, the editor has the possibility to make corrections on deleted or folded parts of the object. Furthermore the degree of accuracy is much higher than in **1b.** Using **1b** the

precision of the vector depends on the homogenous illumination of the microscope slide and on the transparency of the objects. In addition, no software is available which has the capability to trace the outline of an object with overlapping areas (cp. **fig. 2.**).

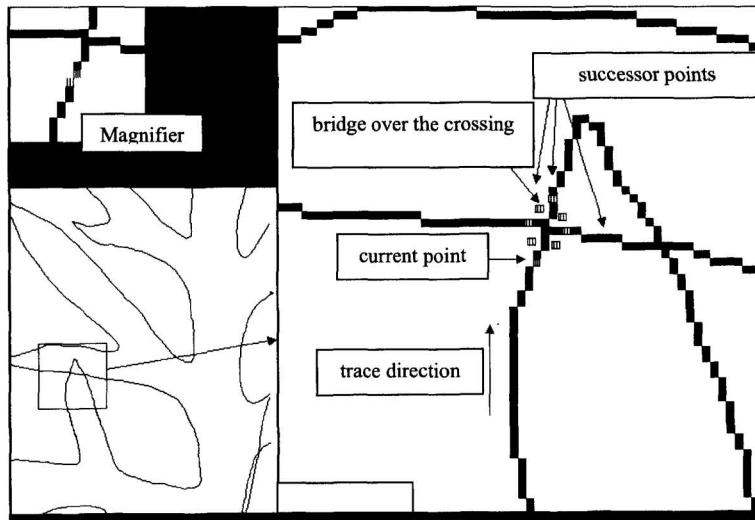


Fig. 1. Screenshot of the conversion from a bitmap into a vector graph. In the bottom left corner you can see a part of a leaflet; on the right a square magnification of an overlapping area and on the top left there is a software magnifier.

Ad 2) The conversion of a bitmap into vector graphs is the crucial point of the method. There are some algorithms, which are used for line tracing [10]. But these algorithms are not suitable for overlapping areas of e.g. secondary segments (cp. **fig. 1.** and **2.**). For this purpose it was necessary to develop a new and interactive algorithm.

For the further processing (e.g. excision of secondary segments or of the ultimate segments (**US**) of leaflets, cp. **fig. 7.- 9.**) it is essential that all points of the vector form an incessant ascending index series. The editor has to fix the starting point (always in the bottom left side of the vector). The algorithm trace the outline throughout time so that there is a white pixel on the left and a black pixel on the right.

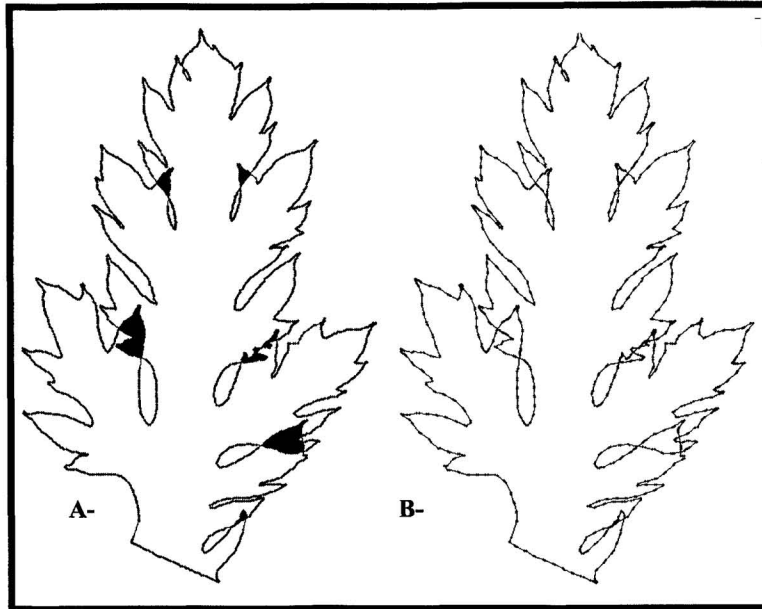


Fig. 2. Vector graph of a leaflet from *Achillea pratensis*. **A-** overlapping areas are black. Vector graph with plotted vector points **A-** with more than 3000 points, **B-** after a thinning with only 1000 points.

Crossings will be detected by a polygonal testfield (cp. **fig. 1.**). If the software recognizes a possible crossing then an alert box appears. If the editor accepts this region as a crossing then he has the possibility to mark the correct following point with the mouse and lead the line tracing algorithm over the cross. Possible gaps in the lines are also detected and can be overbridged. After the conversion the software asks if every or every other point should be used. The editor has to make a compromise between accuracy and available memory. In the standard screen the points are invisible since only the lines between the points are plotted.

Ad 3) and Ad 4) For a proper comparison all vectors have to undergo two different scale transformations. First we arbitrarily established the scaling in the following way. The required size (in pixel) for leaflets is their length (in mm) times 20, for rayflorets it is their length (in μm) divided by 10 (further named as

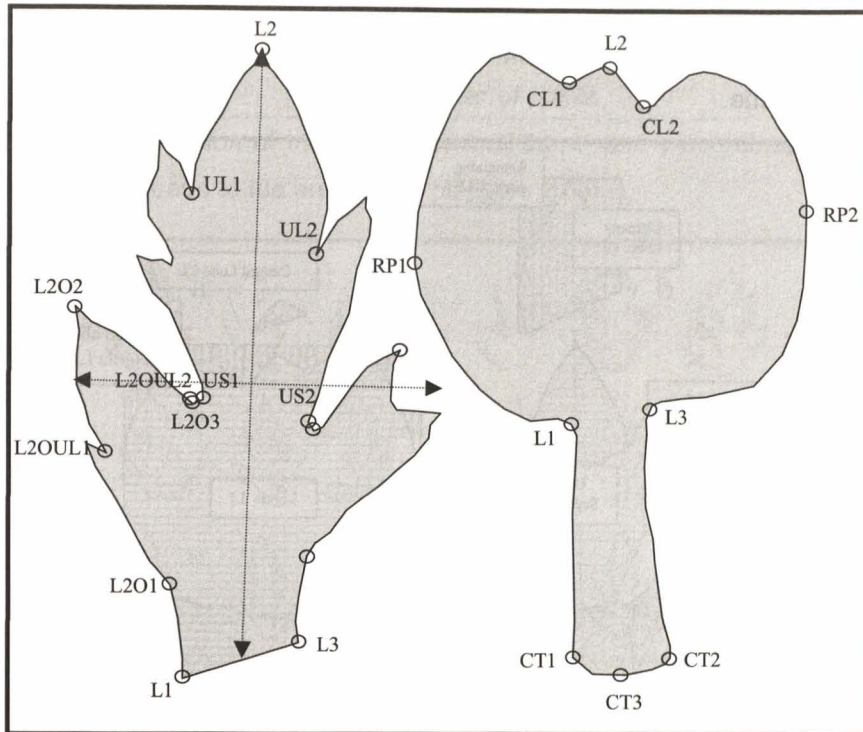


Fig. 3. Position of characteristic points of a leaflet and a rayfloret. Leaflet: **L1**, **L2**, **L3** begin, top and end of the leaflet; **UL1**, **L2**, **UL2** begin, top and end of ultimate lobe; **US1**, **L2**, **US2** begin, top and end of ultimate segment; **L2O1**, **L2O2**, **L2O3** begin, top and end of leaflet 2.order; **L2OUL1**, **L2O2**, **L2OUL2** begin, top and end of ultimate lacinula of leaflet 2.order. Rayfloret: **CT1**, **L2**, **CT2** begin, top and end of the rayfloret; **L1**, **L2**, **L3** begin, top and end of the ligula; **RP1**, **RP2** left and right reversal point; **CL1**, **L2**, **CL2** begin, top and end of central lobe of ligula.

original_sized scale transformation, **fig. 5. A-F**, **6. A-F**). Second, all vectors are resized to the same length (cp. **fig. 5. a-f**, **6. a-f**). All features yielded by this transformation are signed with % (further named as **equal_sized** scale transformation). The pictures of both types of resized vectors are stored as a compressed bitmap for a quick usage on the screen.

Ad 5) An automatic recognition of the structure of the **leaflets** or of the **rayflorets** by the use of an algorithm is not possible. Therefore it is necessary to ask the editor for characteristic points of the object (cp. **fig. 3.**, **4.**). This input is

separated from the measuring procedure, and the information about those points is stored in a separate file. Therefore it is possible to control the position of these points at any time.

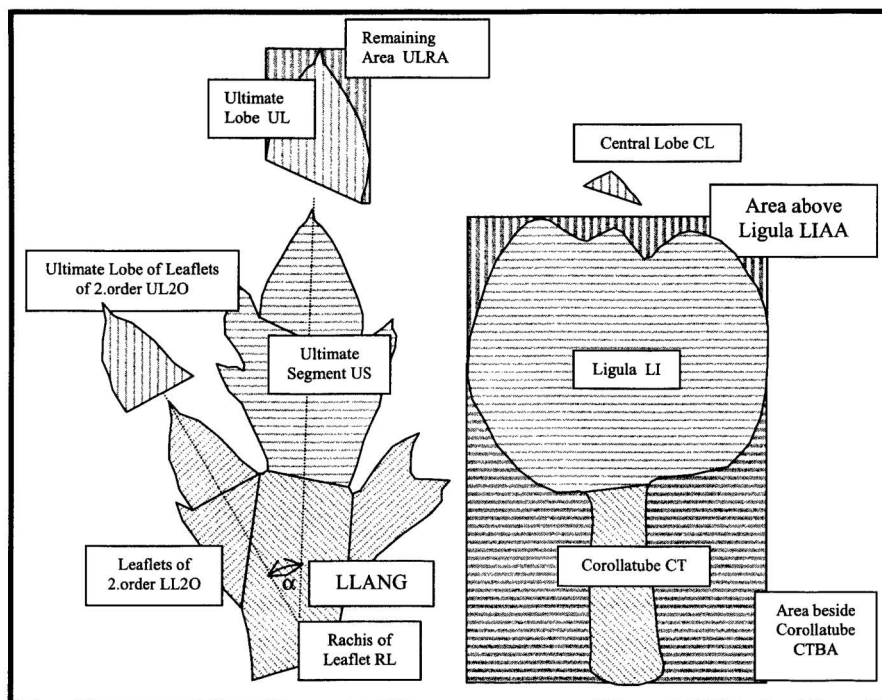


Fig. 4. Position of characteristic points of leaflet and a rayfloret. Explanation of the termini technici – US, UL, ULRA, RL, LL2O, UL2O, LI, LIAA, CL, CT, CTBA, α apex angle of leaflet LLANG remaining area.

Figure 3. shows the position of the characteristic points. Each point must be a point of the vector (cp. **fig. 2.**). This kind of processing ensures that all marked segments of the object can be cut out and stored as separate vector or can be rotated or can be resized (cp. **fig. 8., 9.**).

Ad 6: Before measurement each vector will be resized to a maximum size. This procedure guarantees a maximum precision. After that all high-order segments (cp. **fig. 4.**) will be cut out. The area of each segment are computed according **formula 1.**..The perimeter of segments is the sum of Euclidian distances between

the vector points.

$$A = \left| \sum (x(i) * (y(i+1) - y(i-1))) \right| / 2$$

for $i=1 \dots$ number of points

Formula 1. Computation of the determinant of the x- and y-coordinates from the vector points leads to the area of the polygon.

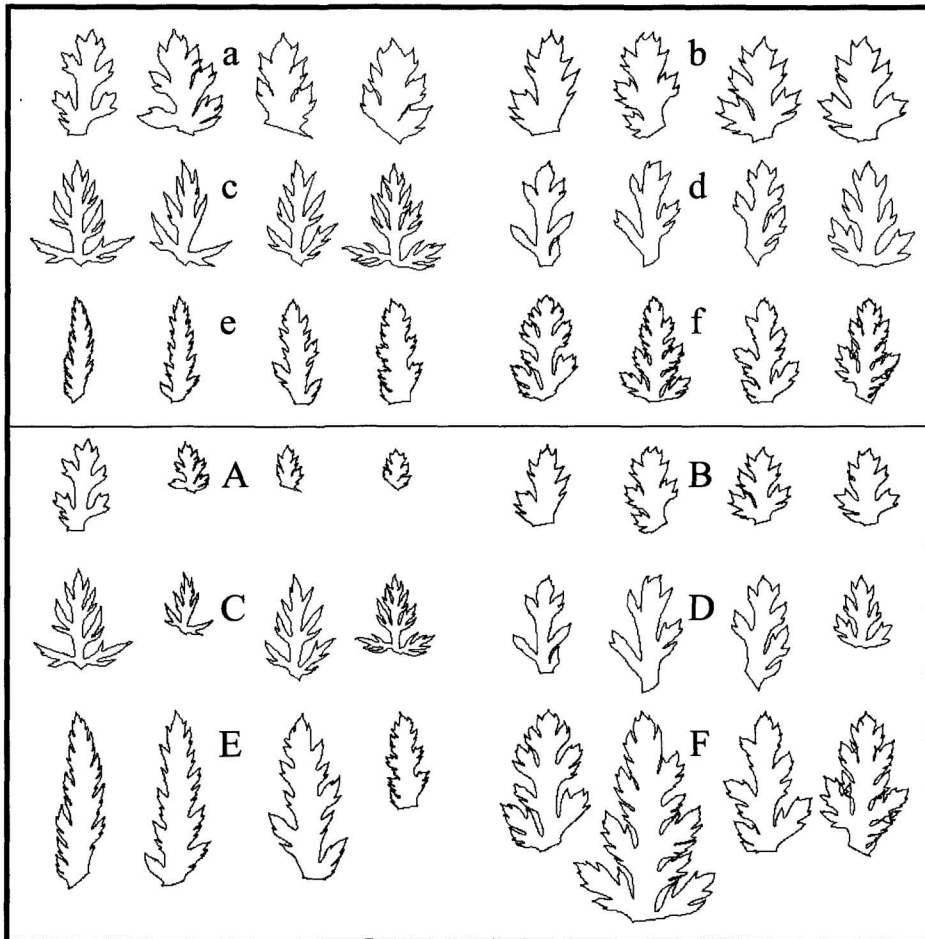


Fig. 5. Primary segments of *Achillea* species - **a, A-** *A. collina*; **b, B-** *A. pannonica*; **c, C-** *A. sudetica* (type SUD_W1, [3]); **d, D-** *A. sudetica* (type SUD_W2, [3]); **e, E-** *A. distans*; **f, F-** *A. pratensis*. Vectorgraphs signed with lower case letters are resized to the same length, signed with upper case letters are correctly sized to each other.

The length L of segments is equal to the Euclidian distance between the top point and the mean of the start point and the end point. The breadth B of segments is equivalent to the breadth of the circumscribed rectangle (lines with an arrow in fig. 3.).

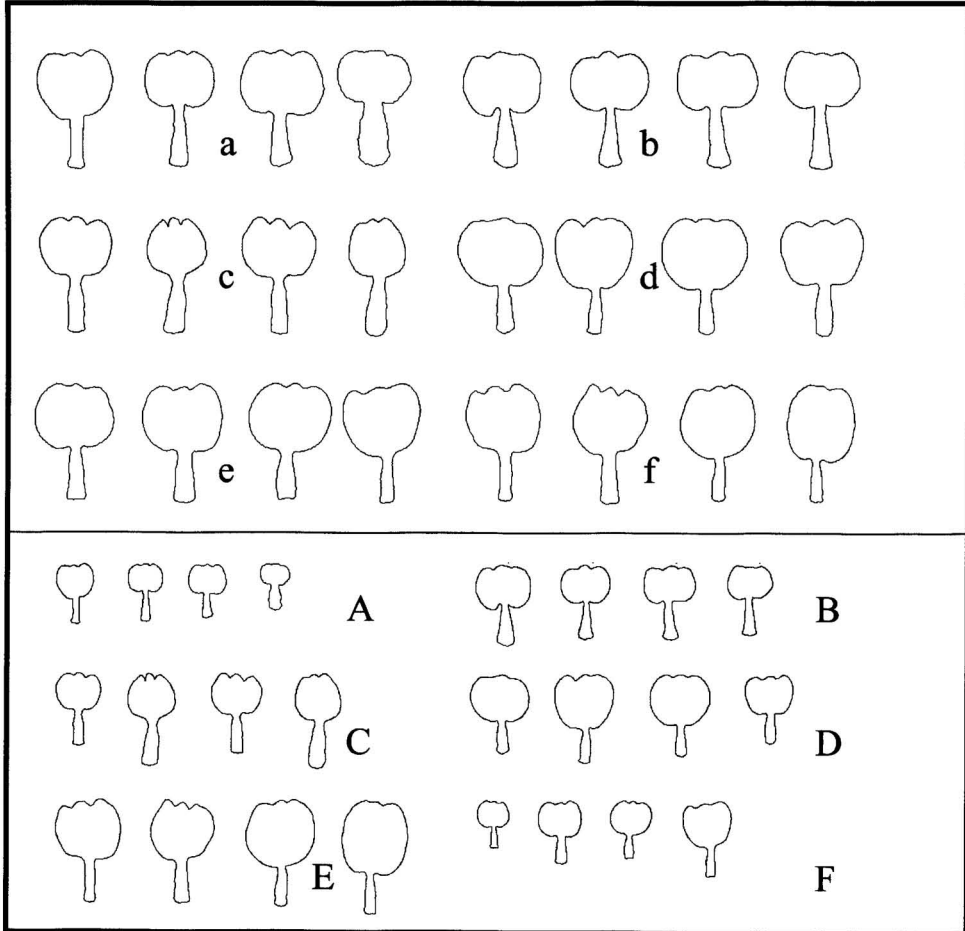


Fig. 6. Rayflorets of *Achillea* species - a, A- *A. collina*; b, B-*A. pannonica*; c, C- *A. sudetica* (type SUD_W1, [3]); d, D- *A. sudetica* (type SUD_W2, [3]); e, E- *A. distans*; f, F- *A. pratensis*. Vectorgraphs signed with lower case letters are resized to the same length, signed with upper case letters are correctly sized to each other.

As one can see in fig. 3., 4. the baseline of the ultimate segment (US) and ultimate lobe (UL), is in most cases oblique. For a better comparison the

DET_MORPH algorithm straightened the baseline (cp. fig. 8., 9.). Both the original shaped and the straightened shaped segments will be measured.

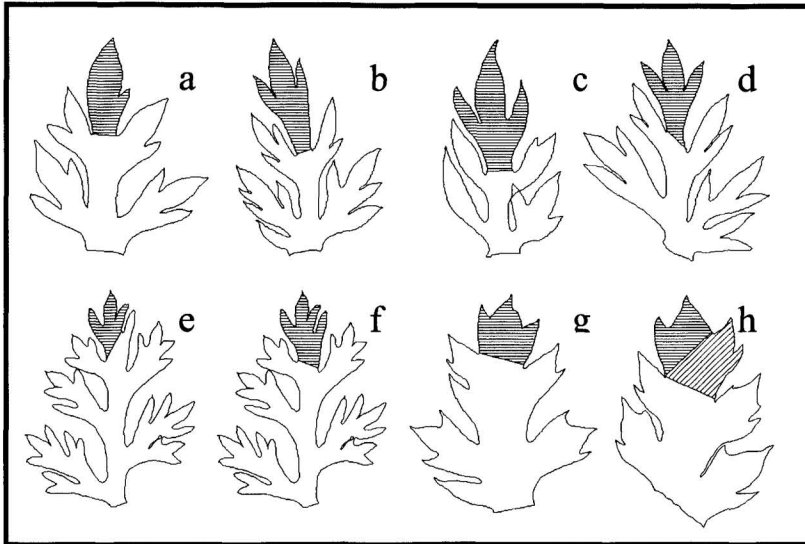


Fig. 7. Various possibilities for the definition of ultimate segments (a - d *A. ceretana*, e, f *A. setacea*, g, h *A. collina*).

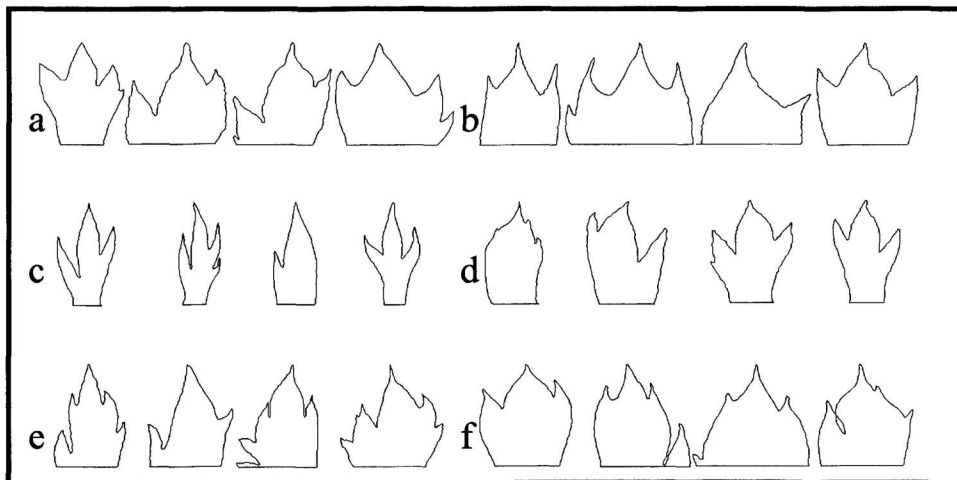


Fig. 8. Ultimate segments of *Achillea* species – a - *A. collina*; b- *A. pannonica*; c - *A. sudetica* (type SUD_W1, [3]); d - *A. sudetica* (type SUD_W2, [3]); e - *A. distans*; f - *A. pratensis*.

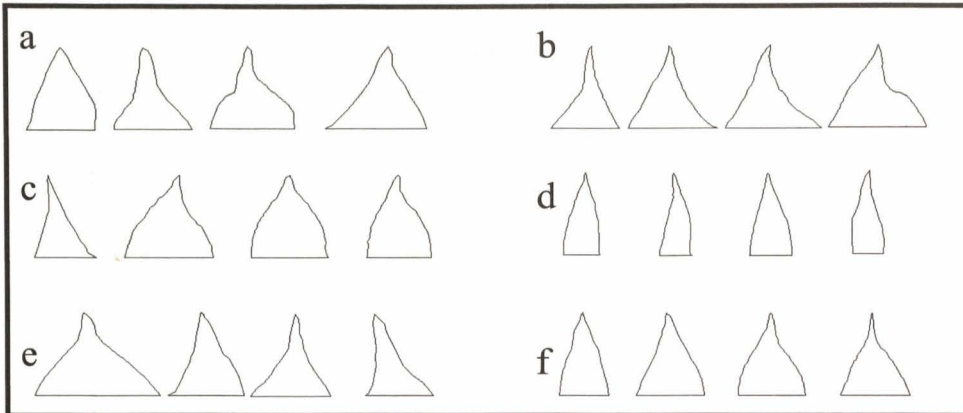


Fig. 9. Ultimate lobes of *Achillea* species – **a** - *A. collina*; **b**- *A. pannonica*; **c** - *A. sudetica* (type **SUD_W1**, [3]); **d** - *A. sudetica* (type **SUD_W2**, [3]); **e** - *A. distans*; **f** - *A. pratensis*.

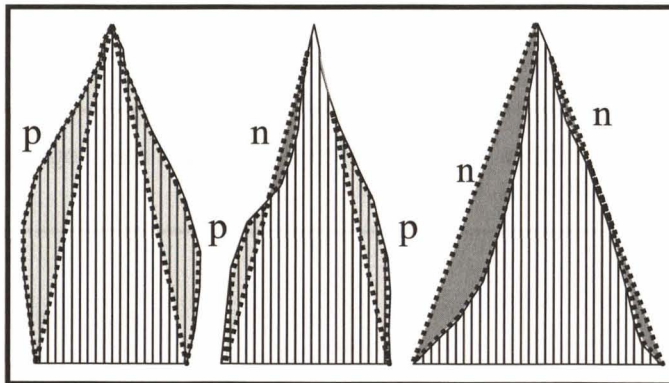


Fig. 10. Automatic registration of the value of concavity or convexity of the ultimate lobes of primary segments; **p** positive area (**ULPA**), **n** negative area (**ULNA**).

The shape of the **UL** of the **leaflets** is an important feature of a differential diagnoses. Therefore it is necessary to obtain a precise information about the concavity or convexity of the outline (**fig. 10**). The algorithm creates on the both sides of the **UL** a polygon. This polygon are on the left or right side of a virtual line between begin and top and also between top and end of the **UL**. After this the areas of the respective polygons are computed. A convexity leads to a positive area (**ULPA** = sum of positive areas left and right), a concavity to a negative area (**ULNA** = sum of negative areas left and right). The features **ULPA** and **ULNA** lead in

relation to the Area of the **Ultimate Lobe UL_A** to the following features (the values are computed by **formula 2. – 4.**

$$\text{CONVEX} = \text{ULNA} * 100 / \text{UL_A}$$

ULNA ... sum of negative areas left and right of the ultimate lobe
UL_A ... area of the ultimate lobe

Formula 2. Computation of the convexity of **UL**.

$$\text{CONCAV} = \text{ULPA} * 100 / \text{UL_A}$$

ULPA ... sum of positive areas left and right of the ultimate lobe
UL_A ... area of the ultimate lobe

Formula 3. Computation of the concavity of **UL**.

$$\text{CONCAV1} = (\text{ULPA} - \text{ULNA}) * 100 / \text{UL_A}$$

ULPA ... sum of positive areas left and right of the ultimate lobe
ULNA ... sum of negative areas left and right of the ultimate lobe
UL_A ... area of the ultimate lobe

Formula 4. Computation of a remaining area **CONCAV1**

The features **Area above Ligula LIAA** and **Area beside Corollatube CTBA** are computed similar to **ULPA** and **ULNA** (cp. **fig. 4.**). For the **LIAA** the algorithm creates a polygon between the left reversal point **RP1** (cp. **fig. 3.**), the top left and top right corner of the circumscribed rectangle, the right reversal point **RP2**, and at least along the outline of the vector between **RP2** and **RP1**. For **CTBA** an analogous procedure works out the respective polygon.

The areas obtained can be related to other areas and lead to the so called remaining areas - **RA**. The values are computed by **formula 5.**

$$\text{RA} = \text{As} * 100 / |\text{Ar} - \text{As}|$$

As ... Area of a segment
Ar ... Area of the circumscribed rectangle

Formula 5. Computation of a remaining area **RA**.

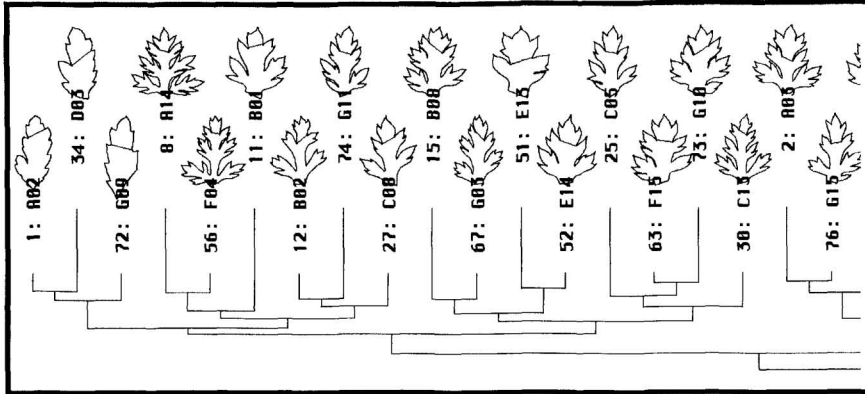


Fig. 11. Part of a dendrogramm from a Cluster analysis. The information about the grouped objects is available with nicknames and graphs.

Some examples are **LLRA**, **RA** of Leaflet; **ULRA**, **RA** of Ultimate Lobe of Leaflet; **USRA**, **RA** of Ultimate Segment of Leaflet; **RFRA**, **RA** of Rayflorete; **LIRA** **RA** of Ligula of Rayflorete; **CTRA** **RA** of Corolla Tube.

Table 1. shows all yielded features of the rayflorete, **tab. 2.** the features of the leaflets.

Abbreviation: perimeter P , area A , length L , breadth B
Rayflorete (without ovary): RF P , RF A , RF L
Ligula of rayflorete: LL P , LL A , LL L , LL B
Central lobe of ligula: CL P , CL A , CL L , CL B
Corolla tube: CT P , CT A , CT L , CT B mean breadth
Area above ligula LIAA
Area beside corolla tube CTBA
Distance between base line and the median of reversal points in per cent of the length of the rayflorete REP%RFL
Remaining area of rayflorete: Rayflorete RFRA , Ligula LIRA , Corolla Tube CTRA

Tab. 1. The features of rayflorete yielded from the **DET_MORPH** algorithm.

Abbreviation: perimeter P , area A , length L , breadth B
Leaflet: LL_P , LL_A , LL_L , LL_B , number of lobes NRLOB
Ultimate lobe: UL_P , UL_A , UL_L , UL_B and with straightened baseline S_ respectively
Rachis of leaflet: LL_RH_P , LL_RH_A , LL_RH_B
Number of segments of second order NRL2O
Ultimate segment: US_P , US_A , US_L , US_B , and with straightened baseline S_ respectively, USNRLOB
Smallest segment, IL2O_P , IL2O_A , IL2O_L , IL2O_B , number of lobes IL2NRLO
Largest segment of second order: ML2O_P , ML2O_A , ML2O_L , ML2O_B , number of lobes ML2NRLO , ultimate lobe: ML2UL_P , ML2UL_A , ML2UL_L , ML2UL_B ,
Median segment of second order: L2O_P , L2O_A , L2O_L , L2O_B , number of lobes L2NRLO
Angle between segment and rachis of leaflet: minimal LL2ANGI , maximal LL2ANGM
Center of gravity from primary segments LL_GP_L , LL_GP_B
Center of gravity from ultimate lobes SUL_GP_L , SUL_GP_B
Center of gravity from ultimate segments SUS_GP_L , SUS_GP_B
Remaining Areas: Leaflet LLRA , Ultimate Lobe ULRA , Ultimate Segment USRA
Convex area of UL – ULPA
Concav area of UL – ULNA

Tab. 2. The features of leaflets yielded from the **DET_MORPH** algorithm.

Results and Discussion

The new software fulfills two major tasks. On the one hand exactly measured values of new features from leaflets and rayflorets are available for taxonomic purpose now. On the other hand the yielded graphs (leaflets – fig. 5., rayflorets – fig. 6., ultimate segment – fig. 8. and ultimate lobe – fig. 9.) can be sorted with arbitrary data, e.g. results of the **MOBCENTR**-algorithm [11] and combined e.g. with a dendrogram of a cluster analysis (fig. 11.). On the basis of such possibilities it is easy to get a clear sight of the data. This leads quickly to a precise interpretation.

For the application of the newly available features in a biosystematic study some important questions should be discussed.

Definition of the ultimate segment (US) of a leaflet of the leaves: A first clue to the use of the ultimate segments is given in [12], however no appropriate

definition can be defined. One useful rule is that most species of the *A.millefolium* group show an ultimate segment with at least 2 to 3 lobes. **Fig. 7.** shows **leaflets** from different species with various possibilities for the definition of ultimate segments. It is evident that the ultimate segment of **e** is 3-lobed but the definition given under **f** may be accepted too. In contrast in **h** we cannot determine exactly which definition is correct. A similar situation is given in **a** to **d**. In most cases (**a** to **d** and **g**, **h**) a clear decision is only possible if one can look on a greater sample of a population! The shape and size of **US** are very important features for the definition of taxa [12].

Shape and size: With the great number of newly available features there is a serious question about the importance of these features [13,14]. Which ones are essential for the description of shape, which are hidden behind the correlation with the size? The now available vector graphs make it possible to compare a plot of **original_sized** with **equal_sized** data from **leaflets** (cp. **fig. 5.**, **6.**). It is obvious that the human recognition favored the size for grouping, but in a biosystematic study, size and shape, both are necessary prerequisites.

We would like to point out that many features show a low correlation between the **equal_sized** and **original_sized** computations. **Fig. 12.** shows a scatterplot from **RF_A** against **CTBA** (correlation coefficient = **0,95**, **n = 616**). If we use the combination **%RF_A** against **CTBA** there is only a poor correlation (correlation coefficient = **- 0,10**, **fig. 13.**).

For the appearance of **leaflets** the number of secondary segments (**NRL20**) and the number of lobes (**NRLOB**) are very important (**fig. 5.**). In the **original_sized** computation **LL_B** shows a moderate correlation with **NRLOB** (**0,64**, **n = 616**) and **NRL20** (**0,55**, **n=616**) further on **NRLOB** and **NRL20** are correlated, too (**0,79**, **n = 616**). The value of the last correlation coefficient is self-explanatory. In contrast the **equal_sized** computation of leaflet breadth **%LL_B** shows **no** correlation with the **original_sized** feature **LL_B** (**0,01**, **n = 616**) and only a poor correlation with **NRLOB** (**- 0,23**, **n = 616**) and **NRL20** (**- 0,22**, **n = 616**).

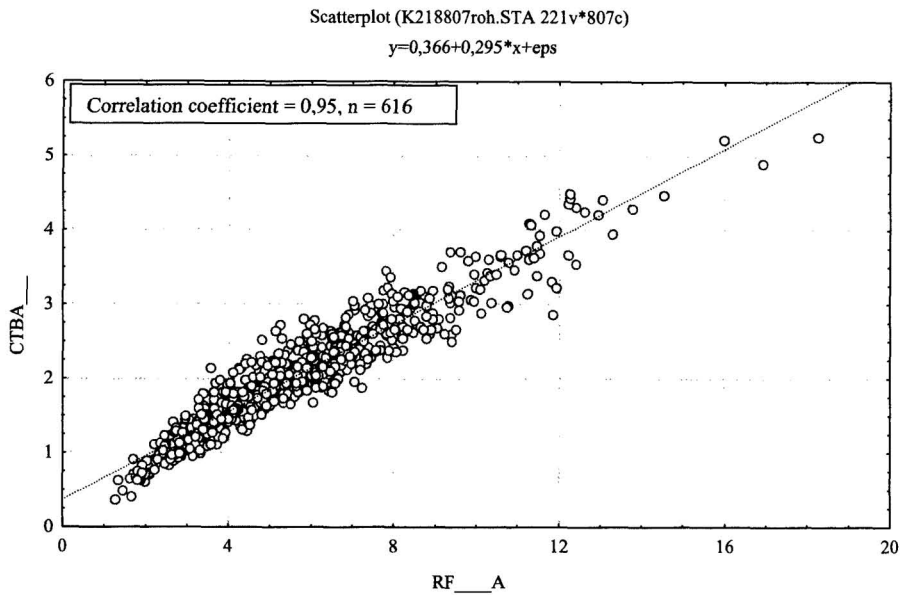


Fig. 12. Scatterplot of n=616 samples of the *A.millefolium* group – Area of rayflore (original_sized) against area beside corolla tube (original_sized).

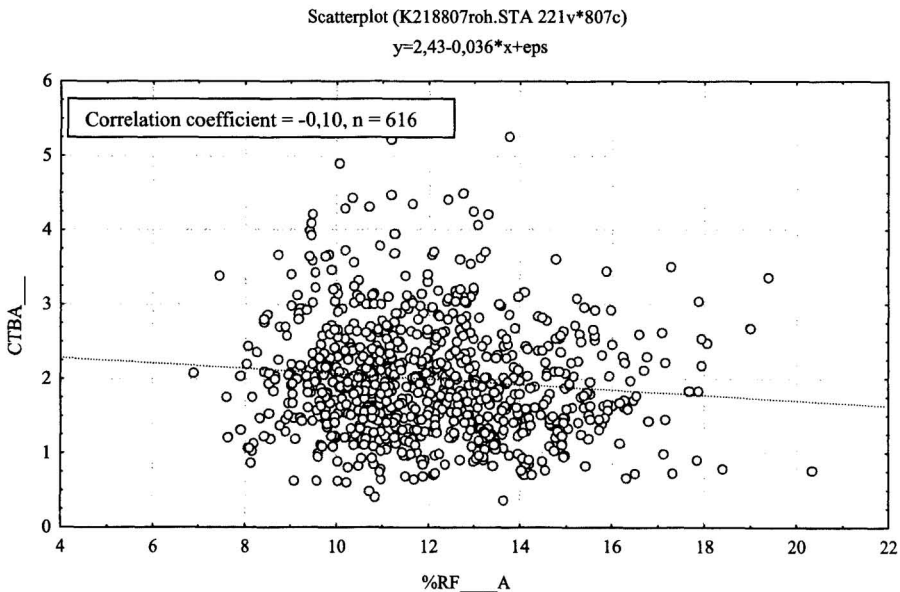


Fig. 13. Scatterplot of n=616 samples of the *A.millefolium* group – Area of rayflore (equal_sized) against area beside corolla tube (original_sized).

Within the features of **original_sized** data of **leaflets** strong correlations are visible between the features from the entire leaflet (perimeter, breadth, length and area) and the mean values of leaflet of second order (perimeter, breadth, length and area) and the values of the greatest segment of second order (perimeter, breadth, length and area). A second group of correlations is visible between features of ultimate lobe, and in a weaker manner against the features of ultimate segments and ultimate lobe of leaflet of second order. The third group of strong correlations is within features of ultimate segments.

At a first glance on features of **equal_sized** data of **leaflets** there are similar groups of stronger correlations but there are also some remarkable differences. The perimeter of the entire leaflet (**LL_P**) is correlated with **NRLOB**, **ML2_P** and **ML2NRLO** only. The ultimate lobes' values and the ultimate segments' values show negative correlations against **NRLOB** and **NRL20**.

Between features of rayflorets there are also strong correlations visible. Three groups of features can be distinguished. First the correlations between **original_sized** features are strong for all features of entire rayfloret, the ligula and the area beside corollatube (**CTBA**). Second all features of ligula, and third all features of central lobe show a strong correlation. In the case of **equal_sized** data there are similar groups visible.

These observations lead to the following conclusion:

The shape of **leaflets** is controlled at least by three groups of genes

- A) leaflet's rachis and segments of second order
- B) ultimate segment
- C) ultimate lobe.

The shape of rayflorets is also controlled at least by three groups of genes:

- A) rayfloret's ligula
- B) rayfloret's corollatube
- C) length and perimeter of the rayfloret's central lobe.

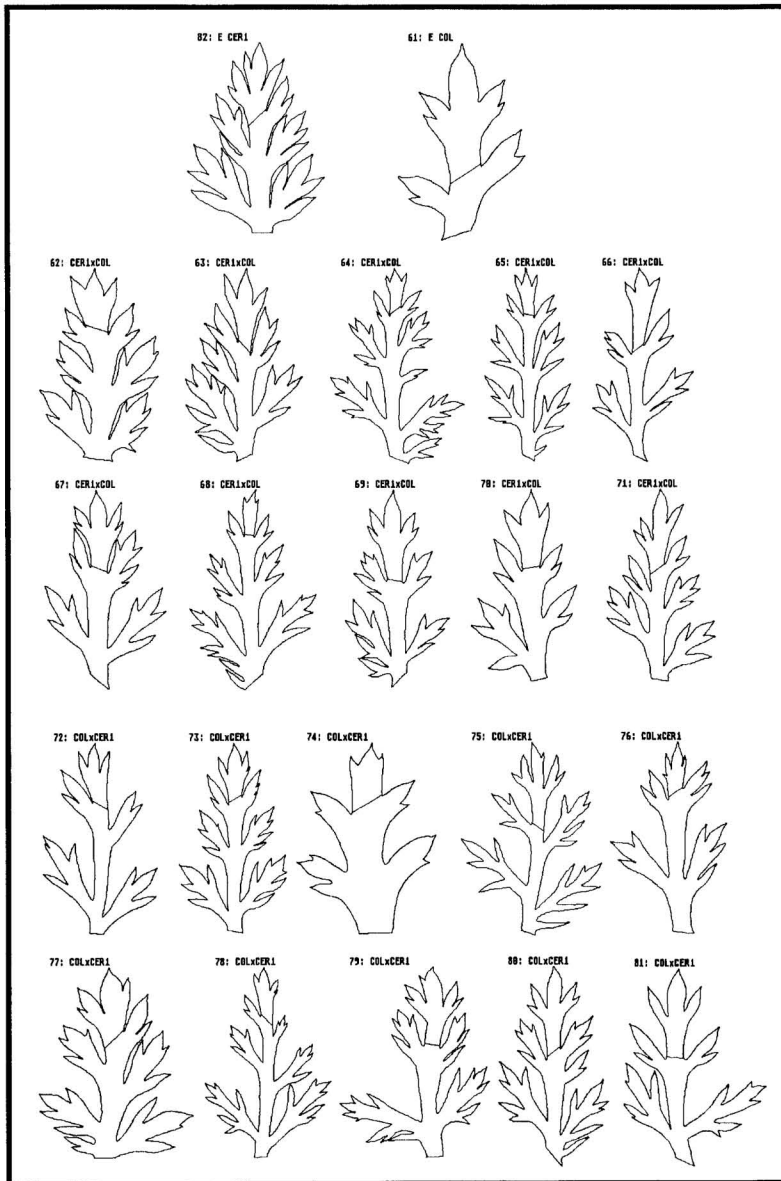


Fig. 14. Primary segments of parents **E CER1** - *A.ceretanica* (4x), **E Col** - *A.collina* (4x) and their crossings: **62 –71** *A.ceretanica* X *A.collina*, **72–81** *A.collina* X *A.ceretanica*.

Next our data analysis was concentrated on the question whether the correlations are similar in all observed species or not. In general the following results can be pointed out:

All species show strong correlations within the above established groups of features in **original_sized** data.

All species reveal their genetic peculiarity in different strongness of correlations in **equal_sized** data only!

All presented results definitely make clear that it is important to use both types of computations, **original_sized** and **equal_sized** but only the **equal_sized** data offer the security to deal with information about shape only.

An additional facility of the **DET_MORPH** algorithm for further pharmacognostic and biosystematic investigations is given: we have graphs from **leaflets** and rayflorets in a database from all studied plants. **Fig. 14.** shows the **leaflets** of tetraploid *A.ceretanica* and *A.collina* and of the filialgeneration of an interbreeding experiment [15]. It is easy to see that only few individuals show a great similarity to *A.collina* [6]. Therefore it is easy to compare in a very detailed manner material from different experiments or various countries. Currently our database on *Achillea* has more than 3000 entries.

Herbarium Specimens

A.collina (n=145): **Austria**- Burg Kreuzenstein, Dürnstein, Unterbergern, Schenkenbrunn, Senftenberg, Rosenberg, Schönberg, Hartenstein, Gütenbachtal, Oberweiden, Retz, Goldene Stiege, **NÖ**, Mauer, Rudolf-Waisenhorngasse, Anton-Krieger-Gasse, Wienerberg (**W**), Winkl (**K**); **Federal Republic of Germany** - Umgebung Düsseldorf; **Slovakia** - Kovacova bei Zvola, Poprad; **Czech Republic**-Hnanize, Pollauer-Berge bei Novi-Rad.

A.setacea (n=8): **Austria** - St.Margareten (**Bgl**).

A.ceretancia (n=4): **France** - St.Fleur.

A.pratensis (n=20): **Austria** - St.Ruprecht ob Murau (**Stmk**)

A.distans s.l. (n=116): **Austria** - Einach, St.Ruprecht ob Murau (**Stmk**), Schellgaden, Burg Moosham (**Sbg**), Pfaffstätten, Baden (**NÖ**), Donnerskirchen (**Bgl**); **Italy** - Groggia,

Friaul Alpe Carnizza, Südtirol Mendel Rabbijoch Tramin, Monte Baldo, **Slovenia** - Plaseggipfel bei Präwald Travnik bei Laibach, Planik-Gipfel; **Slovakia** - Garna Hora, Hohe Tatra; **Romania** - Transsilvania, Siebenbürgen Malojester Hütte, Bucovina Rareu; **Bulgaria** – Rila Mountain; **Switzerland** - Tessin Mt. Generoso.

A.millefolium (inclusive subsp. *Sudetica*; n=258): **Austria** - Oberhüttensee, Wirpitschsee, Tiefenbachsee, Speiereck, Znachtal, Granitzl, Tofern (**Sbg**), Rax and Schneeberg, Ötscher, Irenental (**NÖ**), Fragant, Pöllatal (**K**); **Czech Republic**- Riesengebirge: Schneekoppe, Riesengrund, Kesselgrube; **Italy** – Seiser Alm;

A.annonica (n=75): **Austria** - Braunsberg, Hainburgerberge, Oberweiden (**NÖ**), Bisamberg, Leopoldsberg (**W**); **Romania** - Buftea; **Hungary** - Gyoengyoes, Eger.

References

- [1] Saukel J, Länger R.
Die *Achillea millefolium*-Gruppe (*Asteraceae*) in Mitteleuropa 1.
Phyton 1992; 31: 185-207
- [2] Saukel J.& Länger R.
Die *Achillea millefolium*-Gruppe (*Asteraceae*) in Mitteleuropa, 2.
Phyton 1992; 32: 47-78
- [3] Saukel J.
Achillea.
In: Exkursionsflora von Österreich.
Stuttgart und Wien: Verlag Ulmer, 1994: 813 - 821.
- [4] Wlach W, Saukel J, Kubelka W.
EDV-gestützte Datengewinnung am Beispiel *Achillea*
Sci. Pharm 1995; 63: 341
- [5] Rehberger U.
Pharmakobotanische Untersuchungen an den Trockenrasensippen *Achillea collina* und *Achillea pannonica* aus der *Achillea millefolium*-Gruppe
PhD thesis, University of Vienna, 1996: 1-292
- [6] Bremm M.
Morphologisch-anatomische Untersuchung von Kreuzungsnachkommenschaften tetraploider *Achillea* Sippen
Diploma thesis, University of Vienna, 1998: 1-154
- [7] Nejati S.
Biodiversität südosteuropäischer Schafgarben – Analyse und Nachzucht von Hybridmaterial aus Bulgarien.
PhD thesis, University of Vienna, 2002: 1-277

- [8] Rauchensteiner F.
Biodiversität südosteuropäischer Schafgarben – Analyse von Wildaufsammlungen
PhD thesis, University of Vienna, 2002: 1-337
- [9] Saukel J, Anchev M, Guo Y.-P, Vitkova A, Nedelcheva A, Goranova V, Konakchiev A, Lambrou M, Nejati S, Rauchensteiner F, Ehrendorfer F.
Comments on the Biosystematics of *Achillea* (*Asteraceae-Anthemideae*) in Bulgaria
Phytologia Balcanica 2004; 9: 361-400
- [10] Haberäcker P.
Digitale Bildverarbeitung.
München und Wien, Carl Hanser Verlag, 1987: 1-377
- [11] Saukel J, Länger R.
MOBCENTR: a nonhierarchical classification algorithm for exploratory data analysis (EDA)
Pl. Syst. Evol. 1989;168: 87-94
- [12] Dabrowska J.
Systematic and geographic studies of the genus *Achillea* L. in Poland with special reference to Silesia —
Acta Universitatis wratislaviensis No.419:Prace botaniczne (Wroslav) XXIV, 1982; 1-222
- [13] Humphries J.M, Bookstein F.L, Chernoff B, Smith G.R, Elder R.L, Poss S.G.
Multivariate discrimination by shape in relation to size
Syst. Zool. 1981; 30: 291-303.
- [14] Bookstein F.L.
„Size and Shape“: A Comment on Semantics.
Syst. Zool. 1989; 38: 173-180
- [15] Vetter S, Lambrou M, Franz C, Ehrendorfer F, Saukel J.
Chromosome numbers of experimental tetraploid hybrids and selfpollinated progenies within the *Achillea millefolium* complex (*Compositae*)
Caryologia 1996; 49: 227 - 231